Boundary Integral Equation Neumann-to-Dirichlet Map Method for Gratings in Conical Diffraction

Yumao Wu[1] and Ya Yan Lu[2]

[1]*Department of Electrical and Electronic Engineering, The University of Hong Kong, Pokfulam Road, Hong Kong*

[2]*Department of Mathematics, City University of Hong Kong, Kowloon, Hong Kong*

Boundary integral equation methods for diffraction gratings are particularly suitable for gratings with complicated material interfaces, but are difficult to implement due to the quasi-periodic Green's function and singular integrals at corners. In this paper, the boundary integral equation Neumann-to-Dirichlet map (BIE-NtD) method for in-plane diffraction problems of gratings (Y. Wu and Y. Y. Lu, J. Opt. Soc. Am. A **26**, 2444-2451, 2009) is extended to conical diffraction problems. The method uses boundary integral equations to calculate the so-called Neumann-to-Dirichlet maps for homogeneous sub-domains of the grating, so that the quasi-periodic Green's functions can be avoided. Since wave field components are coupled on material interfaces with the involvement of tangential derivatives, a least squares polynomial approximation technique is developed to evaluate tangential derivatives along these interfaces for conical diffraction problems. Numerical examples indicate that the method performs equally well for dielectric or metallic gratings.

OCIS codes: 050.1755,050.1960,000.4430

1. Introduction

Periodic structures such as diffraction gratings [1–3], photonic crystals and metamaterials are important in numerous applications due to their unusual ability for molding, manipulating and controlling light. Efficient numerical methods are needed in the analysis, design and characterization of these periodic structures. Over the last several decades, many numerical methods have been developed for diffraction gratings and other periodic structures. While general numerical methods, such as the finite-difference time-domain (FDTD) method and the finite element method [4] are extremely versatile, more special methods, such as the Fourier modal method (FMM) [5–7] and the boundary integral equation (BIE) method [8–16] are often more efficient. The FMM is widely used, since it is relatively simple to implement,

but its accuracy may be limited when it is used with a staircase approximation for general material interfaces [17, 18] and it may have convergence problems for highly conducting metallic gratings [19, 20]. The BIE method is suitable for structures with piecewise constant refractive index profiles, but it is relatively complicated to implement, since the integral operators are related to the quasi-periodic Green's function which requires sophisticated lattice sums techniques to evaluate.

For structures which are periodic in one direction and invariant in another direction, in-plane diffraction problems are often studied. In that case, the electromagnetic fields are independent of z (the variable along the invariant direction) and the governing equations (in the frequency domain) are reduced to scalar Helmholtz equations. However, for these periodic structures, it is also important to analyze conical diffraction problems, where the incident waves depend on z as $\exp(i\gamma_0 z)$ for a given non-zero constant γ_0. Under this assumption, the Maxwell's equations are reduced to a system of Helmholtz equations for two components of the electromagnetic fields. For piecewise homogeneous media, these two components are coupled along the material interfaces, involving not only the normal derivatives but also the tangential derivatives. The BIE method is one of the oldest methods for gratings and a formulation for conical diffractions was developed in the early 1970s [8]. However, the combination of the quasi-periodic Green's function, the corner singularities of the electromagnetic fields and the tangential derivatives makes the BIE difficult to implement [16].

In a recent work [21], we developed the so-called boundary integral equation Neumann-to-Dirichlet map (BIE-NtD) method for in-plane diffraction problems. Unlike the traditional BIE method, the BIE-NtD method avoids the quasi-periodic Green's function, and uses the standard Green's function for homogeneous media to define the integral operators. The corner singularities are simply treated with a well-established graded mesh technique. The BIE-NtD method is also capable of analyzing complicated grating structures with many material interfaces. In this paper, we extend the BIE-NtD to conical diffraction problems. The main procedure is similar to the one given in [21], but the interface conditions become more complicated. We approximate the tangential differential operator along the interfaces based on a least squares method with polynomial expansions. Numerical results illustrate that the method is quite efficient for both dielectric and metallic gratings.

2. Problem formulation

We consider a structure which is periodic in the x direction with a period L, finite in the y direction given by $0 < y < D$ for a constant $D > 0$ and invariant in the z direction, where $\{x, y, z\}$ forms a Cartesian coordinate system. The structure is sandwiched between two homogeneous media in the top ($y > D$) and the bottom ($y < 0$). The periodic structure and the surrounding media are specified by a relative permittivity function ε and a relative

magnetic permeability function μ, and they depend only on x and y.

In the top, we specify a plane incident wave that depends on z as $\exp(i\gamma_0 z)$, then the scattered waves have the same z dependence. As a result, we only need to work on the z components of the electromagnetic fields: E_z and H_z. For simplicity, we use $\tilde{H}_z$ which is H_z multiplied by the free space impedance, and denote the column vector of E_z and $\tilde{H}_z$ by $\boldsymbol{u}$. For piecewise homogeneous media, ε and μ are piecewise constant functions, then all six components of the electromagnetic fields satisfy

$$\partial_x^2 u + \partial_y^2 u + \eta\, u = 0 \tag{1}$$

in each homogeneous medium, where $\eta = k_0^2 \varepsilon\mu - \gamma_0^2$, $k_0 = \omega/c$ is the free space wavenumber, c is the speed of light in vacuum, ω is the angular frequency and $\exp(-i\omega t)$ is the assumed time dependence.

The functions E_z and $\tilde{H}_z$ are only coupled on interfaces between different homogeneous media. Let Γ be a material interface, $\boldsymbol{\nu} = (\nu_x, \nu_y)$ be a unit normal vector of Γ, $\boldsymbol{\tau} = (-\nu_y, \nu_x)$ be the unit tangential vector of Γ, then E_z, $\tilde{H}_z$ and

$$\frac{\varepsilon}{\eta}\,\partial_{\boldsymbol{\nu}} E_z + \frac{\gamma_0}{k_0\eta}\,\partial_{\boldsymbol{\tau}} \tilde{H}_z, \quad \frac{\mu}{\eta}\,\partial_{\boldsymbol{\nu}} \tilde{H}_z - \frac{\gamma_0}{k_0\eta}\,\partial_{\boldsymbol{\tau}} E_z \tag{2}$$

must be continuous across Γ.

For $y > D$ and $y < 0$, the homogeneous media have constant relative permittivity and permeability $\{\varepsilon^{(1)}, \mu^{(1)}\}$ and $\{\varepsilon^{(2)}, \mu^{(2)}\}$, respectively, then we can write down the incident wave $\boldsymbol{u}^{(i)}$, the reflected wave $\boldsymbol{u}^{(r)}$ and the transmitted wave $\boldsymbol{u}^{(t)}$ as follows:

$$\boldsymbol{u}^{(i)}(\boldsymbol{r}) = \boldsymbol{a}_0 \exp[i(\alpha_0 x - \beta_0^{(1)} y)], \quad y > D, \tag{3}$$

$$\boldsymbol{u}^{(r)}(\boldsymbol{r}) = \sum_{j=-\infty}^{\infty} \boldsymbol{b}_j \exp[i(\alpha_j x + \beta_j^{(1)} y)], \quad y > D, \tag{4}$$

$$\boldsymbol{u}^{(t)}(\boldsymbol{r}) = \sum_{j=-\infty}^{\infty} \boldsymbol{c}_j \exp[i(\alpha_j x - \beta_j^{(2)} y)], \quad y < 0, \tag{5}$$

where $\boldsymbol{r} = (x, y)$, the z dependence $\exp(i\gamma_0 z)$ is removed for simplicity, $\boldsymbol{a}_0$ is a given vector, $\boldsymbol{b}_j$ and $\boldsymbol{c}_j$ are unknown vectors, α_0 is real and

$$\alpha_j = \alpha_0 + 2\pi j/L, \quad \beta_j^{(p)} = \sqrt{\eta^{(p)} - \alpha_j^2}, \quad \eta^{(p)} = k_0^2 \varepsilon^{(p)} \mu^{(p)} - \gamma_0^2,$$

for any integer j and for $p = 1, 2$.

The diffraction problem can be analyzed on the rectangular domain Σ given by $0 < x < L$ and $0 < y < D$. The periodicity of the structure gives rise to the following quasi-periodic condition:

$$\boldsymbol{u}(x + L, y) = \exp(i\alpha_0 L)\, \boldsymbol{u}(x, y). \tag{6}$$

Meanwhile, we can define two operators $\mathcal{B}^{(1)}$ and $\mathcal{B}^{(2)}$ [22], and write down exact boundary conditions at $y = 0^-$ and $y = D^+$ as

$$\partial_y \boldsymbol{u} = \mathcal{B}^{(2)} \boldsymbol{u}, \qquad y = 0^-, \tag{7}$$

$$\partial_y \boldsymbol{u} = \mathcal{B}^{(1)} \boldsymbol{u} - 2\mathcal{B}^{(1)} \boldsymbol{u}^{(i)}, \quad y = D^+. \tag{8}$$

In the above, $\mathcal{B}^{(1)}$ and $\mathcal{B}^{(2)}$ are 2×2 matrix operators whose diagonal entries are operators $\mathcal{B}_0^{(1)}$ and $\mathcal{B}_0^{(2)}$, respectively. The operator $\mathcal{B}_0^{(1)}$ satisfies

$$\mathcal{B}_0^{(1)} \exp(i\alpha_j x) = i\beta_j^{(1)} \exp(i\alpha_j x), \quad j = 0, \pm 1, \pm 2, ... \tag{9}$$

Similarly, $\mathcal{B}_0^{(2)}$ maps $\exp(i\alpha_j x)$ to $-i\beta_j^{(2)} \exp(i\alpha_j x)$ for all j. In practice, these operators are approximated by matrices.

3. Operator marching scheme

In order to analyze multilayer grating structures, we follow a procedure that manipulates two operators from the bottom ($y = 0^-$) to the top ($y = D^+$). We call this procedure the operator marching scheme. The principle of this scheme was originally developed in [23]. It has been successfully applied to photonic crystal problems [22, 24, 25] and to in-plane diffraction grating problems [21]. The operator marching scheme is similar to the scattering matrix method [26] used in the FMM, but it has more geometric flexibility as demonstrated in [25].

As in our previous work [21], the rectangular domain $\Sigma = \{\boldsymbol{r} = (x, y) \mid 0 < x < L,\ 0 < y < D\}$ that covers one period of the grating is divided into homogeneous sub-domains as shown in Fig. 1, where the sub-domain Ω_j is bounded by two curves Γ_{j-1} and Γ_j, and two

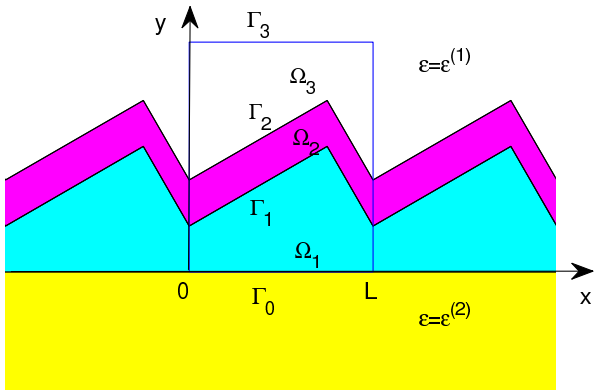

Fig. 1. Rectangular domain Σ for one period of a diffraction grating.

vertical line segments at $x = 0$ and $x = L$. Assuming the total number of sub-domains is m,

then Γ_0 and Γ_m are horizontal line segments at $y = 0$ and $y = D$, respectively. For conical diffraction, we follow our previous work [22] and define operators on the curve Γ_j based on the vector $\boldsymbol{u}$:

$$\mathcal{Q}_j^+ \boldsymbol{u}_j = \partial_{\boldsymbol{\nu}} \boldsymbol{u}_j^+, \quad \mathcal{Q}_j^- \boldsymbol{u}_j = \partial_{\boldsymbol{\nu}} \boldsymbol{u}_j^-, \quad \mathcal{Y}_j \boldsymbol{u}_j = \boldsymbol{u}_0, \tag{10}$$

where $\boldsymbol{u}$ represents the z components of the electromagnetic fields satisfying the quasi-periodic condition (6) and the radiation condition (7), $\boldsymbol{u}_j$ denotes $\boldsymbol{u}$ on Γ_j, $\partial_{\boldsymbol{\nu}} u_j^+$ and $\partial_{\boldsymbol{\nu}} u_j^-$ denote the one-sided limits (from above and below Γ_j, respectively) of the normal derivative of $\boldsymbol{u}$ on Γ_j, ν is the upward normal unit vector of Γ_j. The operators $\mathcal{Q}_j^+$ and $\mathcal{Q}_j^-$ link $\boldsymbol{u}$ on Γ_j to its normal derivative, and the operator $\mathcal{Y}_j$ links $\boldsymbol{u}$ on Γ_j to $\boldsymbol{u}$ on Γ_0.

At $y = 0^-$, since $\boldsymbol{u}$ satisfies the boundary condition (7), we set $\mathcal{Q}_0^- = \mathcal{B}^{(2)}$. Meanwhile, we let $\mathcal{Y}_0 = \mathcal{I}$ where $\mathcal{I}$ is the identity operator. If the two operators $\mathcal{Q}_m^+$ and $\mathcal{Y}_m$ are obtained, we can solve $\boldsymbol{u}$ at $y = D$ from boundary condition (8), i.e.,

$$(\mathcal{Q}_m^+ - \mathcal{B}^{(1)})\boldsymbol{u}_m = -2\mathcal{B}^{(1)} \boldsymbol{u}^{(i)}|_{y=D^+}, \tag{11}$$

and calculate the reflected and the transmitted waves by

$$\boldsymbol{u}^{(r)}|_{y=D^+} = \boldsymbol{u}_m - \boldsymbol{u}^{(i)}|_{y=D^+}, \quad \boldsymbol{u}^{(t)}|_{y=0^-} = \boldsymbol{u}_0 = \mathcal{Y}_m \boldsymbol{u}_m. \tag{12}$$

To find $\mathcal{Q}_m^+$ and $\mathcal{Y}_m$, we need two kinds of operations: (1) propagation steps that calculate $\{\mathcal{Q}_j^-, \mathcal{Y}_j\}$ from $\{\mathcal{Q}_{j-1}^+, \mathcal{Y}_{j-1}\}$ for $j = 1, 2, ..., m$; (2) transition steps that calculate $\mathcal{Q}_j^+$ from $\mathcal{Q}_j^-$ for $j = 0, 1, ..., m$.

The jth propagation step marches the operators from Γ_{j-1} to Γ_j. For photonic crystals, the sub-domains Ω_j ($1 \le j \le m$) are square or hexagon unit cells and we have used the so-called Dirichlet-to-Neumann (DtN) maps of the unit cells to march the operators [22,24,25]. For any u satisfying the Helmholtz equation (1) in Ω_j, the DtN map is the operator Λ_j such that $\Lambda_j u = \partial_{\boldsymbol{\nu}} u$ on the boundary of Ω_j (denoted as $\partial\Omega_j$). In [22,24,25], the DtN maps are constructed using cylindrical wave expansions. For diffraction gratings, the geometry of the sub-domain Ω_j may be quite irregular and the original method developed in [24] for computing Λ_j becomes unreliable. In [21], we developed a BIE method for computing the inverse of the DtN map, i.e., the NtD map $\mathcal{V}_j$, and proposed to use $\mathcal{V}_j$ to complete this step. More precisely, we first write down a BIE relating u and $\partial_{\boldsymbol{\nu}} u$ on the boundary of Ω_j for any u satisfying Eq. (1), and then find the NtD map $\mathcal{V}_j$ by solving that integral equation. The BIE requires some modification for domains with corners and it can be solved by a well-established Nyström method with a kernel-splitting technique [27, 28]. Since the field components satisfy the quasi-periodic condition (6), we can further eliminate u and $\partial_{\boldsymbol{\nu}} u$ on the vertical boundary segments of $\partial\Omega_j$ and obtain the reduced NtD map $\mathcal{N}_j$ satisfying

$$\mathcal{N}_j \begin{bmatrix} \partial_{\boldsymbol{\nu}} u_{j-1}^+ \\ \partial_{\boldsymbol{\nu}} u_j^- \end{bmatrix} = \begin{bmatrix} \mathcal{N}_{j,11} & \mathcal{N}_{j,12} \\ \mathcal{N}_{j,21} & \mathcal{N}_{j,22} \end{bmatrix} \begin{bmatrix} \partial_{\boldsymbol{\nu}} u_{j-1}^+ \\ \partial_{\boldsymbol{\nu}} u_j^- \end{bmatrix} = \begin{bmatrix} u_{j-1} \\ u_j \end{bmatrix}, \tag{13}$$

where $\mathcal{N}_j$ is also given in 2×2 blocks. For conical diffraction problems, the two components in $\boldsymbol{u}$ are coupled. Consequently, the marching formulae given in [22] must be revised as

$$\mathcal{Z} = \left(\mathcal{I} - \begin{bmatrix} \mathcal{N}_{j,11} & \\ & \mathcal{N}_{j,11} \end{bmatrix} \mathcal{Q}_{j-1}^{+}\right)^{-1} \begin{bmatrix} \mathcal{N}_{j,12} & \\ & \mathcal{N}_{j,12} \end{bmatrix}, \tag{14}$$

$$Q_j^{-} = \left(\begin{bmatrix} \mathcal{N}_{j,22} & \\ & \mathcal{N}_{j,22} \end{bmatrix} + \begin{bmatrix} \mathcal{N}_{j,21} & \\ & \mathcal{N}_{j,21} \end{bmatrix} \mathcal{Q}_{j-1}^{+}\mathcal{Z}\right)^{-1}, \tag{15}$$

$$\mathcal{Y}_j = \mathcal{Y}_{j-1}\mathcal{Z}\mathcal{Q}_j^{-}. \tag{16}$$

The jth transition step performs the transition for operator $\mathcal{Q}$ passing through the interface Γ_j. From the continuity of E_z, $\tilde{H}_z$ and the two functions given in (2), we obtain

$$\mathcal{Q}_j^{+} = \begin{bmatrix} \sigma_1 & 0 \\ 0 & \sigma_2 \end{bmatrix} \mathcal{Q}_j^{-} + \begin{bmatrix} 0 & \sigma_3\,\partial_{\boldsymbol{\tau}} \\ \sigma_4\,\partial_{\boldsymbol{\tau}} & 0 \end{bmatrix}, \tag{17}$$

where $\partial_{\boldsymbol{\tau}}$ is the tangential derivative operator along Γ_j, σ_1, σ_2, σ_3 and σ_4 are the following functions defined on Γ_j:

$$\sigma_1 = \frac{\varepsilon^{-}\eta^{+}}{\varepsilon^{+}\eta^{-}}, \quad \sigma_2 = \frac{\mu^{-}\eta^{+}}{\mu^{+}\eta^{-}}, \quad \sigma_3 = \frac{\gamma_0(\eta^{+}-\eta^{-})}{k_0\eta^{-}\varepsilon^{+}}, \quad \sigma_4 = -\frac{\gamma_0(\eta^{+}-\eta^{-})}{k_0\eta^{-}\mu^{+}}. \tag{18}$$

In the above, the superscripts $+$ and $-$ denote one-sided limits towards Γ_j from above and below, respectively. As a special case, we notice that for in-plane diffraction problems, $\gamma_0 = 0$, $\sigma_1 = \mu^{+}/\mu^{-}$ and $\sigma_2 = \varepsilon^{+}/\varepsilon^{-}$, $\sigma_3 = \sigma_4 = 0$, $\partial_{\boldsymbol{\tau}}$ disappears and Eq. (17) becomes the continuity of $\mu^{-1}E_z$ and $\varepsilon^{-1}\tilde{H}_z$. For conical diffraction, it is necessary to evaluate the tangential derivative operator.

In a numerical implementation, if the curve Γ_j is discretized by N_j points for $0 \le j \le m$, then the operators $\mathcal{Q}_j^{+}$ and $\mathcal{Q}_j^{-}$ are approximated by $(2N_j)\times(2N_j)$ matrices, $\mathcal{Y}_j$ is approximated by an $(2N_0)\times(2N_j)$ matrix, $\mathcal{N}_j$ becomes an $(N_{j-1}+N_j)\times(N_{j-1}+N_j)$ matrix, the functions σ_1, σ_2, σ_3 and σ_4 are represented by $N_j\times N_j$ diagonal matrices, and $\partial_{\boldsymbol{\tau}}$ should be approximated by an $N_j\times N_j$ matrix. Therefore, the operator marching scheme involves a sequence of matrix manipulations.

4. Graded mesh and tangential derivative

As it is evident from Fig. 1, the sub-domains Ω_j $(1 \le j \le m)$ have corners even when the physical interfaces are smooth. In the BIE approach for computing the NtD map $\mathcal{V}_j$, a graded mesh is used to discretize $\partial\Omega_j$ [21]. It is introduced to smooth out the field singularities at the corners, so that a standard Nyström method for discretizing the integral operators can be applied [27]. The method is pure numerical and relatively simple to implement, since analytic properties of electromagnetic fields at corners are not needed. If $\partial\Omega_j$ is originally parameterized by a parameter t (which should scale well with the arclength), the graded

mesh is obtained from a change of variable $t = w(s)$ and a uniform discretization in s. The function w depends on an integer $p \geq 2$, such that the derivatives of w up to order $p-1$ vanish at the corners. This implies that the density of the discretization points is much higher near the corners than the density in other places.

The graded mesh causes some inconvenience in the first and last steps of the operator marching scheme. At $y = 0^-$, we need to initialize $\mathcal{Q}_0^-$ as $\mathcal{B}^{(2)}$. Since $\mathcal{Q}_0^-$ must be compatible with the NtD map of Ω_1, it should be discretized on a graded mesh. However, $\mathcal{B}^{(2)}$ is best discretized on a uniform mesh in x, since it is related to the Rayleigh expansion (Fourier series) of $\boldsymbol{u}^{(t)}$ given in (5). In [21], we tackled this problem by a least squares method. A matrix $\boldsymbol{S}$ is introduced, such that

$$\mathcal{B}^{(2)} = \boldsymbol{S}\tilde{\mathcal{B}}^{(2)}\boldsymbol{S}^{\dagger}, \tag{19}$$

where $\boldsymbol{S}^{\dagger}$ is the pseudoinverse of $\boldsymbol{S}$, $\mathcal{B}^{(2)}$ and $\tilde{\mathcal{B}}^{(2)}$ denote matrix approximations of the same operator on the graded mesh and the uniform mesh, respectively. For the last step, we first transform $\mathcal{Q}_m^+$ and $\mathcal{Y}_m$ from the graded mesh to the uniform mesh by

$$\tilde{\mathcal{Q}}_m^+ = \boldsymbol{S}^{\dagger}\mathcal{Q}_m^+\boldsymbol{S}, \quad \tilde{\mathcal{Y}}_m = \boldsymbol{S}^{\dagger}\mathcal{Y}_m\boldsymbol{S}, \tag{20}$$

and then find the solutions using Eqs. (11) and (12) on the uniform mesh.

If Γ_j is a true physical interface, it is necessary to perform the transition step (17) which calculates $\mathcal{Q}_j^+$ from $\mathcal{Q}_j^-$. The step involves the tangential derivative operator $\partial_{\boldsymbol{\tau}}$ along Γ_j. If Γ_j is given in parametric form as

$$\boldsymbol{r} = \boldsymbol{r}(t) = (x(t), y(t)), \tag{21}$$

and if the tangent vector $\boldsymbol{\tau}$ is in the increasing t direction, then

$$\partial_{\boldsymbol{\tau}} u(\boldsymbol{r}) = \frac{1}{|\boldsymbol{r}'(t)|}\frac{du(\boldsymbol{r}(t))}{dt}, \tag{22}$$

where $|\boldsymbol{r}'(t)| = \sqrt{|x'(t)|^2 + |y'(t)|^2}$. Clearly, the tangential derivative is easily obtained from the derivative with respect to t. In an actual numerical computation, Γ_j is discretized by N_j points, therefore we look for an $N_j \times N_j$ matrix $\boldsymbol{T}_j$ that approximates $\partial_{\boldsymbol{\tau}}$. Notice that if Γ_j consists of more than one smooth segments separated by corner points, $\boldsymbol{T}_j$ should be a block diagonal matrix where each diagonal block corresponds to one smooth segment.

Consider a smooth segment of Γ_j given by the parametric representation (21) for $t_0 \leq t \leq t_{q+1}$. The graded mesh on the segment corresponds to $\{t_0, t_1, t_2, ..., t_q, t_{q+1}\}$, where q is the number of interior points on the segment, $\boldsymbol{r}(t_0)$ and $\boldsymbol{r}(t_{q+1})$ are the end points of the segment (also corner points of Γ_j). To simplify the notation, we denote $u(\boldsymbol{r}(t))$ and $du(\boldsymbol{r}(t))/dt$ by $u(t)$ and $u'(t)$, respectively. When the NtD map of the domain Ω_j (or Ω_{j+1}) is approximated

by a matrix, the corner points are removed [21]. Therefore, we only have u at q interior points (t_l, $1 \le l \le q$) and we want to approximate u' at these points.

Standard finite difference formulae for derivatives give only low order of accuracy. More importantly, since the graded mesh is severely clustered near the corner points, round-off errors render the difference formulae unacceptable near the two end points. Our approach is to first approximate $u(t)$ by a polynomial of t using a least squares method, then approximate u' by the derivative of that polynomial. For better numerical stability, we expand the approximant in Chebyshev polynomials. More precisely, the least squares problem is

$$\min_{c_0,c_1,\ldots,c_n} \sum_{l=1}^{q} \left| \sum_{k=0}^{n} c_k T_k(\tilde{t}_l) - u(t_l) \right|^2, \tag{23}$$

where n ($n < q$) is the degree of the approximant, T_k is the Chebyshev polynomial of degree k and $\tilde{t}_l = -1 + 2(t_l - t_0)/(t_{q+1} - t_0)$. The coefficients c_0, c_1, ..., c_n can be solved in terms of $u(t_l)$ for $1 \le l \le q$, then the derivative can be evaluated by

$$u'(t_l) \approx \frac{2}{t_{q+1} - t_0} \sum_{k=0}^{n} c_k T_k'(\tilde{t}_l). \tag{24}$$

The final result can be written as

$$\frac{\partial}{\partial \boldsymbol{\tau}} \begin{bmatrix} u(t_1) \\ u(t_2) \\ \vdots \\ u(t_q) \end{bmatrix} \approx \boldsymbol{C} \begin{bmatrix} u(t_1) \\ u(t_2) \\ \vdots \\ u(t_q) \end{bmatrix}, \quad \boldsymbol{C} = \boldsymbol{C}_0 \boldsymbol{C}_2 \boldsymbol{C}_1^{\dagger}, \tag{25}$$

where $\boldsymbol{C}_0$ is a diagonal matrix with entries $2/[(t_{q+1} - t_0)|\boldsymbol{r}'(t_l)|]$ for $1 \le l \le q$, $\boldsymbol{C}_1$ and $\boldsymbol{C}_2$ are $q \times (n+1)$ matrices with entries $T_k(\tilde{t}_l)$ and $T_k'(\tilde{t}_l)$ (for $0 \le k \le n$ and $1 \le l \le q$), respectively, and $\boldsymbol{C}_1^{\dagger}$ is the pseudoinverse of $\boldsymbol{C}_1$. In our numerical implementation, the polynomial degree n is typically chosen to be around $q/2$.

5. Numerical examples

In this section, we demonstrate our method by a few numerical examples. All examples involve only non-magnetic media, thus the relative magnetic permeability is $\mu = 1$. The first example is a sinusoidal dielectric grating previously studied by a number of authors [16, 29, 30]. As shown in Fig. 2, a sinusoidal interface separates air and a homogeneous dielectric medium with relative permittivity $\varepsilon = 4$. The period and the groove depth of the grating are L and $d = 0.3L$, respectively. The incident wave vector forms a 75° angle with the z axis, and its projection in the xy plane forms a 60° angle with the y axis. The free space wavelength of the incident wave is $\lambda = 0.5L$. The vector amplitude $\boldsymbol{a}_0$ of the incident wave is chosen so that its second component (for $\tilde{H}_z$) is zero.

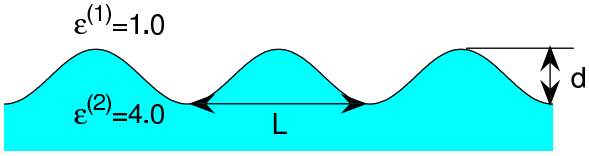

Fig. 2. A dielectric sinusoidal diffraction grating.

Table 1. Diffraction efficiencies of a sinusoidal grating in a conical mounting obtained by the the C method, the BIE method [16], and the BIE-NtD method.

Order	C method	BIE method	This work
R_{-3}	0.1121×10^{-1}	0.1121×10^{-1}	0.11211×10^{-1}
R_{-2}	0.3741×10^{-1}	0.3741×10^{-1}	0.37410×10^{-1}
R_{-1}	0.3873×10^{-1}	0.3873×10^{-1}	0.38728×10^{-1}
R_0	0.1033	0.1033	0.10330
T_{-5}	0.1858×10^{-3}	0.1855×10^{-3}	0.18580×10^{-3}
T_{-4}	0.2466×10^{-4}	0.2482×10^{-4}	0.24663×10^{-4}
T_{-3}	0.7396×10^{-2}	0.7394×10^{-2}	0.73957×10^{-2}
T_{-2}	0.4922×10^{-1}	0.4922×10^{-1}	0.49215×10^{-1}
T_{-1}	0.9925×10^{-1}	0.9923×10^{-1}	0.99250×10^{-1}
T_0	0.7146×10^{-1}	0.7145×10^{-1}	0.71463×10^{-1}
T_1	0.5183	0.5183	0.51831
T_2	0.6351×10^{-1}	0.6351×10^{-1}	0.63507×10^{-1}

In Table 1, we list the numerical results for diffraction efficiencies computed using the BIE method [16], the coordinate transformation method (C method) [31] (also listed in [16]) and our method. The first column of Table 1 is a list of reflected and transmitted diffraction orders. The agreement between the coordinate transformation method and our method is excellent. In fact, the results for diffraction order T_{-4} suggest that the agreement may be up to 10^{-8}. The agreement between the BIE method and the other two methods is also very good, but the results for T_{-4} and T_{-5} indicate that the agreement is limited to 10^{-6}. Earlier results in [29] and [30] appear to have three correct digits. For T_1, the diffraction efficiencies given in [29] and [30] are 0.5181 and 0.51845, respectively.

The graded mesh on a smooth segment has the property that the mesh size at the middle of the segment is about one half of the ratio between the length of the segment and the

total number of points. For a domain with a few smooth boundary segments, the number of points on each segment may be chosen in proportion to its length. To obtain the results in Table 1, we use a rectangular domain Σ with two sub-domains Ω_1 and Ω_2. Although the interface is smooth, both Ω_1 and Ω_2 have corners. The NtD maps of these two sub-domains are calculated by discretizing their boundaries with a graded mesh of 250 points. The parameter that specifies the graded mesh is $p = 5$. A larger p gives a higher order of convergence, but when p is too large, the problem become ill-conditioned and there will be a loss of precision. On the top and bottom edges (i.e., Γ_2 and Γ_0), the number of points in the graded mesh are $N_2 = N_0 = 49$. A uniform mesh of 25 points is also used on Γ_0 and Γ_2 for connecting the homogeneous media below Γ_0 and above Γ_2, respectively. On Γ_1, we evaluate the tangential derivative based on a polynomial approximation with a polynomial degree $n = 49$.

The second example is a metallic lamellar grating shown in Fig. 3. It has been previously

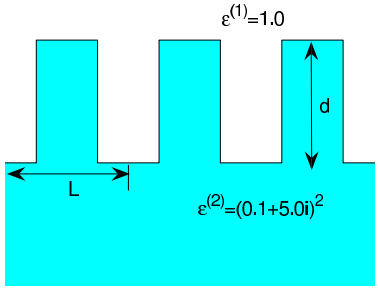

Fig. 3. A metallic lamellar diffraction grating.

analyzed by an analytic modal method [32] and a BIE method [16]. The groove depth is related to the period of the grating as $d = L$. The metal is assumed to have a relative permittivity $\varepsilon = (0.1 + 5.0i)^2$ and the medium above the interface is air. The free space wavelength of the incident wave is $\lambda = 0.5L$ (thus $k_0 = 4\pi/L$). The incident wave vector is $(\alpha_0, -\beta_0^{(1)}, \gamma_0) = k_0(\sqrt{2}/4, -\sqrt{3}/2, \sqrt{2}/4)$. This implies that the angle between the z axis and the wave vector is $\arccos(\sqrt{2}/4) \approx 69.30°$, and the angle between the y axis and the projection of the incident wave vector on the xy plane is $\arctan(1/\sqrt{6}) \approx 22.21°$. The vector amplitude of the incident wave is $\boldsymbol{a}_0 = (2 + \sqrt{3}, 2 - \sqrt{3})^T$. In Table 2, we show numerical results for reflected diffraction efficiencies obtained by the FMM, the BIE method [16] and our method for comparison. A good agreement between the FMM and our method is obtained. The FMM results are obtained using 900 Fourier modes based on the implementation described in [5]. Our results are obtained using a rectangular domain Σ with two homogeneous sub-domains Ω_1 and Ω_2. Each of these two sub-domains has eight corners. The NtD maps of Ω_1 and Ω_2

Table 2. Diffraction efficiencies of a metallic lamellar grating in a conical mounting calculated using the FMM, the BIE method [16] and the BIE-NtD method.

Order	FMM	BIE method	This work
R_{-2}	0.07555	0.0752	0.07556
R_{-1}	0.13265	0.1325	0.13265
R_0	0.44158	0.4427	0.44158
R_1	0.31110	0.3105	0.31112

are calculated by discretizing their boundaries using 840 points. The parameter used in the graded mesh is $p = 5$. On the top and bottom edges Γ_2 and Γ_1, we use $N_2 = N_0 = 119$ points in the graded mesh and 42 points in the uniform mesh. The tangential derivatives on Γ_1 are obtained using polynomials of degree from 28 to 59.

The third example is a metallic echelette grating shown in Fig. 4. The relative permittivity

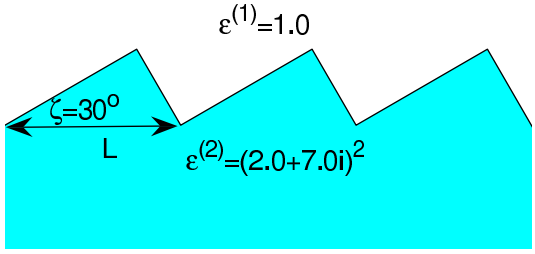

Fig. 4. A metallic echelette diffraction grating.

of the metal is $\varepsilon = (2.0 + 7.0i)^2$ and the medium above the interface is air. The period and the blaze angle of the echelette grating are L and 30°, respectively. As in [33] and [16], we consider an incident wave with a free space wavelength $\lambda = 0.5L$. The incident wave vector forms a 50° angle with the z axis, and its projection in the xy plane is parallel to the y axis. In Table 3, we show reflected diffraction efficiencies for two cases where the vector amplitude of the incident wave is given by $\boldsymbol{a}_0 = (1, 0)^T$ (case 1) and $\boldsymbol{a}_0 = (0, 1)^T$ (case 2), respectively. The results obtained by the coordinate transformation method and the BIE method [16] are also listed for comparison, and they agree reasonably well with our results. In particular, the BIE method and our method give relatively close results. In our implementation, the rectangular domain Σ is divided into two homogeneous sub-domains each having five corners. The NtD maps of these two sub-domains are calculated by discretizing their boundaries with

Table 3. Diffraction efficiencies of a metallic echelette grating in a conical mounting obtained by the C method, the BIE method [16] and the BIE-NtD method.

Case	Order	C method	BIE method	This work
1	R_{-1}	0.5315	0.5315	0.53144
	R_0	0.1751	0.1748	0.17484
	R_1	0.0942	0.0944	0.09445
2	R_{-1}	0.1299	0.1297	0.12961
	R_0	0.2849	0.2845	0.28446
	R_1	0.2477	0.2481	0.24818

600 points. A graded mesh is used with a parameter $p = 5$. On the top and bottom edges Γ_2 and Γ_0, we have 99 points for the graded mesh and 35 points for the uniform mesh. Tangential derivatives along Γ_1 are evaluated from polynomial approximations with polynomial degree from 49 to 99.

6. Conclusion

In this paper, we extended the boundary integral equation Neumann-to-Dirichlet map (BIE-NtD) method, originally developed for in-plane diffraction problems of gratings [21], to conical diffraction problems. The BIE-NtD method retains the main advantages of existing BIE methods for gratings, but avoids the quasi-periodic Green's functions which are tedious to evaluate. The boundary integral equations are used to compute the so-called Neumann-to-Dirichlet maps and they are discretized by a standard Nyström method using a graded mesh for domains with corners. An operator marching scheme is also used so that multilayer grating structures with many interfaces can be easily handled. For conical diffraction, field components are coupled on interfaces corresponding to discontinuities of the material parameters and tangential derivatives must be evaluated along these interfaces. We developed a least squares polynomial approximation method for evaluating the tangential derivatives. Numerical examples indicate that the method is fairly accurate for both dielectric and metallic gratings with or without sharp corners.

Acknowledgments

This research was partially supported by a grant from the Research Grants Council of Hong Kong Special Administrative Region, China (Project No. CityU 102008).

References

1. R. Petit, ed., Electromagnetic Theory of Gratings (Speinger-Verlag, Berlin, 1980).
2. G. Bao, L. Cowsar, and W. Masters, ed., Mathematical Modeling in Optical Sciences (Society for Industrial and Applied Mathematics, 2001).
3. M. Nevière and E. Popov, Light Propagation in Periodic Media (Marcel Dekker, Inc. 2003).
4. G. Bao, Z. M. Chen, and H. J. Wu, "Adaptive finite-element method for diffraction gratings," J. Opt. Soc. Am. A **22**, 1106-1114 (2005).
5. P. Lalanne and G. M. Morris, "Highly improved convergence of the coupled-wave method for TM polarization," J. Opt. Soc. Am. A **13**, 779-784 (1996).
6. G. Granet and B. Guizal, "Efficient implementation of the coupled-wave method for metallic lamellar gratings in TM polarization," J. Opt. Soc. Am. A **13**, 1019-1023 (1996).
7. L. Li, "Use of Fourier series in the analysis of discontinuous periodic structures," J. Opt. Soc. Am. A **13**, 1870-1876 (1996).
8. D. Maystre, Sur la Diffraction et l'Absorption par les Réseaux Utilisés dans l'Infrarouge, le Visible et l'Ultraviolet (PhD dissertation, Université d'Aix-Marseille III, France, 1974).
9. D. Maystre, "Integral Methods," in *Electromagnetic Theory of Gratings*, R. Petit, ed. (Speinger-Verlag, Berlin, 1980), Chapter 3.
10. A. Pomp, "The integral method for coated gratings – computational cost," J. Mod. Opt. **38**, 109-120 (1991).
11. B. H. Kleemann, A. Mitreiter, and F. Wyrowski, "Integral equation method with parametrization of grating profile - Theory and experiments," J. Mod. Opt. **43**, 1323-1349 (1996).
12. D. W. Prather, M. S. Mirotznik, and J. N. Mait, "Boundary integral methods applied to the analysis of diffractive optical elements," J. Opt. Soc. Am. A **14**, 34-43 (1997).
13. E. Popov, B. Bozhkov, D. Maystre, and J. Hoose, "Integral method for echelles covered with lossless or absorbing thin dielectric layers," Appl. Opt. **38**, 47-55 (1999).
14. T. Magath and A. E. Serebryannikov, "Fast iterative, coupled-integral-equation technique for inhomogeneous profiled and periodic slabs," J. Opt. Soc. Am. A **22**, 2405-2418 (2005).
15. A. Rathsfeld, G. Schmidt, and B. H. Kleemann, "On a fast integral equation method for diffraction gratings," Commun. Comput. Phys. **1**, 984-1009 (2006).
16. L. I. Goray and G. Schmidt, "Solving conical diffraction with integral equations," J. Opt. Soc. Am. A **27**, 585-597 (2010).
17. E. Popov, M. Nevière, B. Gralak, and G. Tayeb, "Staircase approximation validity for

arbitrary-shaped gratings," J. Opt. Soc. Am. A **19**, 33-42 (2002).
18. I. Gushchin and A. V. Tishchenko, "Fourier modal method for relief gratings with oblique boundary conditions," J. Opt. Soc. Am. A **27**, 1575-1583 (2010).
19. N. M. Lyndin, O. Parriaux, and A. V. Tishchenko, "Modal analysis and suppression of the Fourier modal method instabilities in highly conductive gratings," J. Opt. Soc. Am. A **24**, 3781-3788 (2007).
20. K. M. Gundu and A. Mafi, "Reliable computation of scattering from metallic binary gratings using Fourier-based modal methods," J. Opt. Soc. Am. A **27**, 1694-1700 (2010).
21. Y. Wu and Y. Y. Lu, "Analyzing diffraction gratings by a boundary integral equation Neumann-to-Dirichlet map method," J. Opt. Soc. Am. A **26**(11), 2444-2451 (2009).
22. Y. Wu and Y. Y. Lu, "Dirichlet-to-Neumann map method for analyzing periodic arrays of cylinders with oblique incident waves," J. Opt. Soc. Am. B **26**, 1442-1449 (2009).
23. Y. Y. Lu and J. R. McLaughlin, "The Riccati method for the Helmholtz equation," J. Acoust. Soc. Am. **100**(3), 1432-1446 (1996).
24. Y. Huang and Y. Y. Lu, "Scattering from periodic arrays of cylinders by Dirichlet-to-Neumann maps," J. Lightwave Technol. **24**, 3448-3453 (2006).
25. Y. Wu and Y. Y. Lu, "Dirichlet-to-Neumann map method for analyzing interpenetrating cylinder arrays in a triangular lattice," J. Opt. Soc. Am. B **25**, 1466-1473 (2008).
26. L. Li, "Formulation and comparison of two recursive matrix algorithms for modeling layered diffraction gratings," J. Opt. Soc. Am. A **13**, 1024-1035 (1996).
27. D. Colton and R. Kress, Inverse Acoustic and Electromagnetic Scattering Theory, 2nd ed. (Springer-Verlag, Berlin, 1998).
28. L. Wang, J. A. Cox, and A. Friedman, "Modal analysis of homogeneous optical waveguides by the boundary integral formulation and the Nyström method," J. Opt. Soc. Am. A **15**, 92-100 (1998).
29. S. L. Chuang and J. A. Kong, "Wave scattering from a periodic dielectric surface for a general angle of incidence," Radio Sci. **17**, 545-557 (1982).
30. L. Li, "Multilayer modal method for diffration gratings of arbitrary profile, depth, and permittivity," J. Opt. Soc. Am. A **10**, 2581-2591 (1993).
31. L. Li, J. Chandezon, G. Granet, and J. P. Plumey, "Rigorous and efficient grating-analysis method made easy for optical engineers," Appl. Opt. **38**, 304-313 (1999).
32. L. Li, "A modal analysis of lamellar diffraction gratings in conical mountings." J. Mod. Opt. **40**, 553-573 (1993).
33. M. Mansuripur, L. Li, and W.-H. Yeh, "Diffraction Gratings: Part 2," Optics & Photonics News **10**, 44-48 (1999).